Spinal decompression sickness: hydrophobic protein and lamellar bodies in spinal tissue

B. A. HILLS

Department of Physiology, University of New England, Armidale, N.S.W. 2351, Australia

Hills BA. Spinal decompression sickness: hydrophobic protein and lamellar bodies in spinal tissue. Undersea & Hyperbaric Med 1993; 20(1):3–16.—Four basic studies have addressed the question of why the spinal cord is so vulnerable to decompression injury, with symptoms exceeding those related to the brain by a ratio often quoted as 3:1. Hydrophobic protein (HP) was discovered in sheep spinal tissue at roughly 3 times (3.3:1) the level in brain and several orders of magnitude greater than in skeletal muscle or plasma. Extravascular lamellar bodies (LBs) of largely phospholipid (PL) were also demonstrated in spinal tissue by electron microscopy using a special fixative, the population being 4.1 times that in brain tissue where some LBs were found adjacent to vascular endothelium. Extracts of spinal surfactant (HP + PL) were found to be particularly surface active on the Langmuir trough, with the HP greatly accelerating monolayer equilibration, especially the recruitment of PL to a rapidly expanding air-aqueous interface. The PL/HP surfactant complex was found to render surfaces hydrophobic when they were able to initiate "strings" of bubbles in supersaturated solutions of gases. These results are discussed as favoring the concept of autochthonous bubbles causing spinal decompression injury exacerbated by the large quantities of spinal surfactant present.

decompression sickness, hydrophobic protein, lamellar bodies, myelination, spinal injury, surfactant

The tendency for paraplegia to occur in preference to other CNS symptoms of DCS, in both divers and caisson workers, has been on record since the work of Bert (1). Moreover, in reviewing more than 200 neurologic cases arising in pearl divers operating off the northern coast of Western Australia around 1909, Blick (2) describes how, at autopsy, most of the 60 deaths could be attributed to respiratory impairment consistent with "a characteristic teased appearance" of spinal tissue in the lower cervical area. This particular vulnerability of the cord, together with the debilitating nature of such decompression injuries, has led to much interest in the mechanism of spinal DCS.

Despite showing gas distending a myelin sheath in sections of the cord of a goat dying under pressure and recording the formation of gas as extravascular, perhaps

incorrectly (3), Boycott and co-workers (4) still endorsed the embolic mechanism first suggested by Bert (1). For many years it was generally accepted that spinal DCS was part of one general category of neurologic or type II DCS caused by arterial bubbles. This theory was not challenged until comparatively recently when Hallenbeck et al. (5) pointed out how spinal exceed cerebral symptoms by a ratio of 3:1 and yet the brain receives some 75–85 times more blood flow (6) and should therefore receive proportionately more arterial bubbles, although regional spinal perfusion rates can vary widely (7). They support this position most convincingly by emphasizing how, in known blood-borne disorders such as fat embolism or subacute bacterial endocarditis, the brain is the major target organ with spinal cord involvement not exceeding 0.4% (8). Hallenbeck et al. (5) therefore looked for a site of occlusion other than the arterial system and presented pathologic evidence to support their contention that cord lesions could occur by obstruction of the vertebral venous system by a combination of bubbles and the degradation products of blood–bubble interaction. More recently there has been a revival of interest in the concept of arterial embolism (3, 9), and the epidemiology of spinal vs. cerebral lesions continues to be a subject of debate.

Hills and James (10) argued against *any* embolic mechanism on the grounds that the symptoms of spinal DCS are not only reversed by recompression but are *repeatedly* pressure reversible, recurring upon decompression in toto with the same distribution (11). It is very difficult to explain the extent of reversal by any embolic mechanism because any intravascular bubbles are known to be cleared when blood flow is restored by recompression (12, 13). The vital issue that remains is why the spinal cord is so much more vulnerable than the brain. It would seem that either the vessels are unique in their ability to arrest circulating bubbles or spinal tissue is much more prone to the separation of gas from solution in extravascular sites. If the spinal cord *is* more prone to the formation of autochthonous bubbles, then the question arises as to what agents might be present to promote such growth. The cord has a high proportion of white-to-gray matter in some vertebrae, especially T4 and L1, where the supersaturation by nitrogen should be high during decompression, but then the same argument should apply to some areas of the brain.

This study represents the culmination of a search for some factor that might promote bubble growth in spinal tissue, departing from traditional emphasis on the driving force (degree of supersaturation) by considering the kinetics. The separation of gas from solution requires the formation of much new interfacial area and, hence, the provision of much energy in the form of surface energy (14). This requirement for surface energy can be reduced considerably by a surfactant locating at the interface when it can greatly facilitate expansion of that interface, especially if recruitment is rapid. Such energy considerations are also implicated in bubble nucleation, as discussed later.

A common example of a very rapidly expanding air–aqueous interface occurs in vivo with the switch from liquid to air breathing at birth, when there is not only a highly potent surfactant present in the form of dipalmitoyl phosphatidylcholine (DPPC), but its rate of recruitment to the surface is increased by 1–2 orders of magnitude by the presence of certain proteins (15). This system enables the air–aqueous interface in the neonate to expand from 2 cm^2 to about 30,000 cm^2 within a few minutes. The combination of DPPC and protein—predominantly the more potent hydrophobic proteins SP-B and SP-C (16)—is known in pulmonary physiology simply as "surfac-

tant" and is produced in the lung by alveolar type II cells as "lamellar bodies" (17). Although hydrophobic protein has been considered unique to the lung (16), this study has been designed to test for its presence—and that of lamellar bodies—in spinal tissue and, for comparison purposes, in brain and other tissues less prone to DCS.

MATERIALS AND METHODS

Principles

In the lung there is about 10% protein in lamellar bodies (18) of which by far the most active in promoting the recruitment of phospholipid to an air–aqueous interface are SP-B and SP-C (19), representing about 28 and 22%, respectively, of the total protein content (16). These proteins are so hydrophobic that they are soluble in chloroform and other lipid solvents (16) so that they are co-extracted with phospholipids upon solvent extraction. In the first study of spinal tissue, the protein in the solvent extract was hydrolyzed to its component amino acids by a standard biochemical technique (20) and the total amino acid estimated photometrically by the standard method of Moore and Stein (21).

In the second study, a sample of the extract was deposited as a monolayer on the pool of a Langmuir trough (Fig. 1) to test for surface activity in the manner conventionally applied to lung surfactant (22).

In a third minor study, the extract of DPPC and hydrophobic protein (HP) was dissolved in chloroform and applied to a clean glass surface, placed in water saturated with air, and then decompressed to test for any propensity to produce bubbles.

In the fourth study, sections of spinal cord were examined for lamellar bodies by electron microscopy using a special fixation procedure (23) by which tannic acid was substituted for most of the glutaraldehyde used conventionally to optimize the resolution of any lamellated surface-active phospholipid (SAPL) present (24).

Materials

The source of material was five adult ewes killed painlessly by stunning with a captive-bolt gun followed by exsanguination. The spinal cord was excised within 15

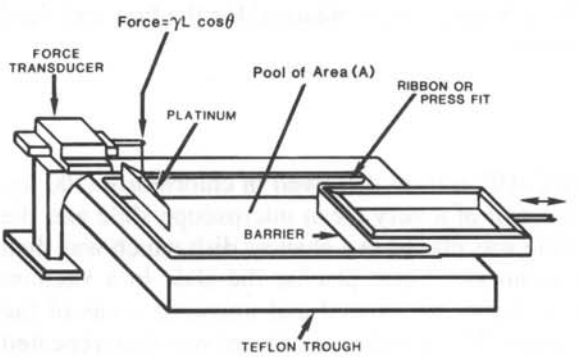

FIG. 1—The Langmuir trough widely used to study surfactant monolayers at an air–aqueous interface. The moveable barrier enables the surface area to be changed by a ratio of up to 10:1 while surface tension (gamma) is continuously monitored as the force with which a clean platinum flag is pulled into the pool.

min of death. Four samples were taken from each cord for electron microscopy, and two other samples were taken at random for histologic examination by light microscopy to ensure no detectable abnormality in the material used. The remainder of the cord was weighed and immediately placed in a vortex blender for homogenization. Samples were also taken from the brain, skeletal muscle, and blood from which plasma was obtained.

Protein analysis

The homogenate from each cord was mixed with 10 times its volume of chloroform:-methanol (2:1), homogenized, and then the lipid solution was separated by centrifugation and the solvent evaporated with N_2. The residue was re-dissolved in chloroform, and samples were set aside for evaluation of surface activity and the ability to promote bubble formation. The remainder was divided into four roughly equal samples, concentrated by evaporating off most of the chloroform with N_2 and then placing 50 μl into a hard glass tube to which is added 1 ml of 6 N.HCl. Each tube was then sealed in vacuo and autoclaved for 24 h at 110°C. The tubes were then opened and the HCl evaporated off. Standard procedure was followed in estimating the amino acid content by adding ninhydrin preparation after the sample was buffered with citric acid and sodium nitrate to pH 5. The concentration was determined using a spectrophotometer at $\gamma = 570$ nm. Blanks were prepared omitting the spinal sample and the absorbance calibrated using a range of known concentrations of bovine serum albumin (BSA). Thus all results were expressed as an equivalent weight of BSA per unit mass of tissue or blood. The identical procedure was followed for brain, plasma, and muscle samples from the same sheep. Total phospholipid was estimated by the standard method of Rouser et al. (25) whereby all organic phosphorus is oxidized to phosphate and determined colorimetrically.

Surface activity

One of the samples of the chloroform extract from the cord was applied to the surface of a pool of saline in a Langmuir trough fabricated from Teflon (Fig. 1) and the solvent allowed to evaporate for 30 min. The surface tension (γ) was monitored continuously by the dipping-plate (Wilhelmy) method as the Teflon barrier was cycled to provide a standard change in surface area (A) of 5:1, generally considered necessary to reach minimum γ values (26). The γ:A loops were obtained for the first and third cycles as direct tests of surface activity.

Bubble formation

Another sample (1 ml) of the DPPC–HP extract dissolved in chloroform (100 μg/ml) was placed on an area (2.5 × 2.5 cm) of a very clean microscope slide and the solvent allowed to evaporate. The slide was placed in a shallow dish which was then filled with water equilibrated with room air. Upon placing the slide in a vacuum desiccator and pulling a vacuum of 0.5 atm, the coated and uncoated areas of the slide were observed for bubble formation. This simple experiment was then repeated using soda water.

Electron microscopy

Two blocks were cut from each sample of spinal tissue for transverse sectioning. Each was fixed for 72 h in glutaraldehyde (1%) plus tannic acid (3%), buffered at a pH of 7.4 with 0.1 *M* sodium cacodylate at 4°C, and rendered isotonic with blood from that animal by adding NaCl to minimize osmotic fluxes. Postfixation was effected with 1% osmium tetroxide buffered at a pH of 7.4 with embedding in resin (Spurr mix 'A', Probing & Structure, Kirwan, QLD) polymerized at 60°C. Particularly thin (<60 nm) sections were cut with a very sharp diamond knife to help resolve any lamellated structure.

RESULTS

Protein hydrolysis

The results of the protein hydrolysis for samples from spinal tissue, muscle, brain, and plasma are summarized in Table 1. It can be seen that the quantity of hydrophobic protein is about 2 orders of magnitude higher in spinal tissue than in muscle, which is almost as low as plasma. A statistical analysis shows that there may be no HP in plasma or muscle because the absorbance of the blanks is almost equal to that of the tests. However, the presence of HP in spinal tissue is highly significant ($P < 0.001$) and almost as significant in brain ($P < 0.002$). The results of the phospholipid analyses are also given in Table 1.

Surface activity

The chloroform extract from the spinal cord proved to be particularly surface active, immediately reducing surface tension from 72 to 24 dyn/cm (mN/m), even before the barrier of the Langmuir trough was moved. Upon compressing the mono-

Table 1: Analysis of Tissues for HP and Phospholipin (PL).

Tissue	Hydrophobic Protein, Equivalent BSA per g tissue	Phospholipid, Equivalent DPPC per g tissue	HP:PL Ratio, Equivalent BSA Equivalent DPPC
Spinal cord	5.46 mg	4.29 mg	0.62
Brain	1.65 mg	1.43 mg	0.60
Skeletal Muscle	0.19 mg	0.20 mg	0.95
Plasma	<0.01 mg	0.012 mg	–
Lung	(2.02 mg)	7.95 mg	0.09–0.42[a]
Spinal: brain ratio	3.3	3.0	–

[a]Data from Oosterlaken-Dijksterhuis et al. (16).

layer, the surface tension remained almost constant (Fig. 2). Upon expansion, the surface tension again remained almost constant at a value very close to the equilibrium surface tension for DPPC of 24 dyn/cm (27). This was quite remarkable compared with monolayers of lung surfactant or pure DPPC, also shown in Fig. 2.

Wetting and bubble formation

The slide coated with the chloroform extract of DPPC–HP proved hydrophobic, displaying a contact angle (θ) of over 90° when water was placed on it, whereas the clean glass displayed a contact angle of less than 5°.

The decompressed slide immersed in water displayed many more bubbles per unit area over the DPPC–HP-coated portion than over the clean area by a ratio of about 10:1. Roughly the same ratio was observed when the slide was placed in soda water. Another interesting difference was the formation of rising bubbles as continuous "strings," but only from the DPPC–HP-coated areas.

Electron microscopy

Sections of the spinal cord revealed many densely osmiophilic inclusions, particularly in the white matter (Fig. 3). At greater magnification most of these proved to be classical lamellar bodies (Fig. 4) as seen in the lung (17), whereas others were vesicles often lining vacuoles (Fig. 5). These differ greatly from myelinated axons as seen in Fig. 6. A count of sequential sections displayed 14.2 lamellar bodies per 10^3 μl—not one intravascular. This compared quite markedly with brain, where a count showed 3.5 per 10^3 μl. A marked difference in the brain was the number of intravascular lamellar bodies—often in endothelial crevices (Fig. 7)—and various other forms of lamellated structures (Fig. 8) often integrated into the oligolamellar lining reported previously (28).

DISCUSSION

The surprising feature of the results is the very large quantity of hydrophobic protein present in spinal tissue, an amount comparable to that in the lung on a weight

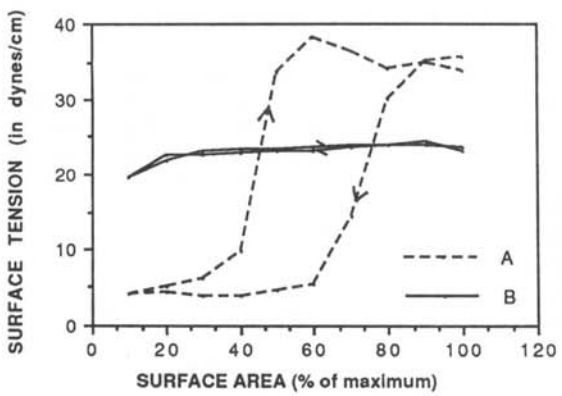

FIG. 2—The relationship between surface tension (γ) and surface area (A) of the pool of the Langmuir trough when the monolayers are placed at the air–aqueous interface are: A, an extract of spinal "surfactant" and, for comparison; B, pure DPPC which is the surface-active ingredient of lung surfactant. Lung rinsings behave the same as B (22).

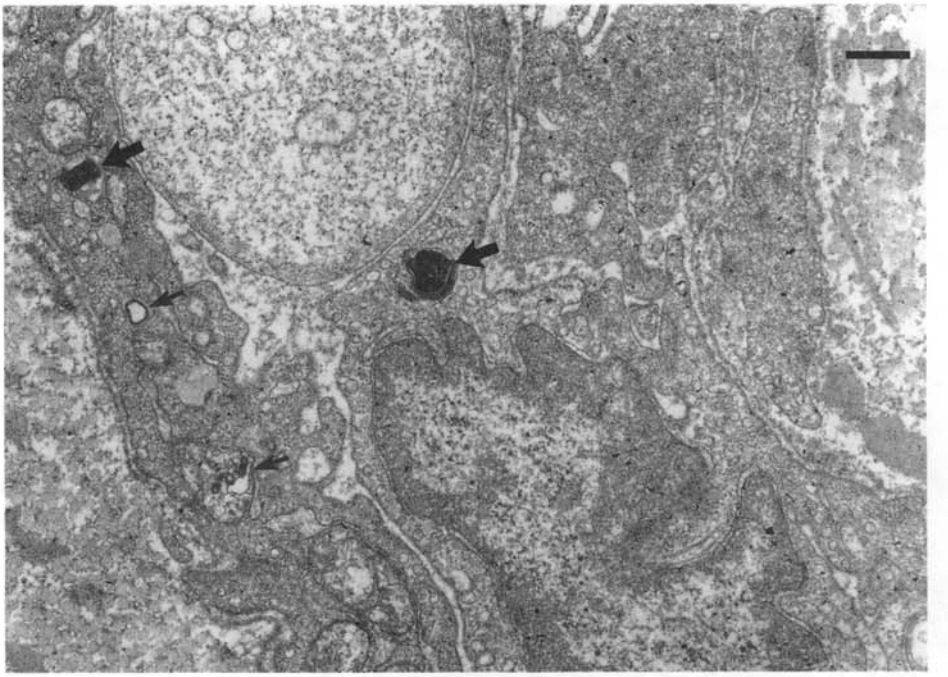

FIG. 3—An electron micrograph of sheep spinal tissue showing two lamellar bodies (*large arrows*) and other lamellated materail (*small arrows*) in perivascular sites of white matter. *Bar* = 500 nm.

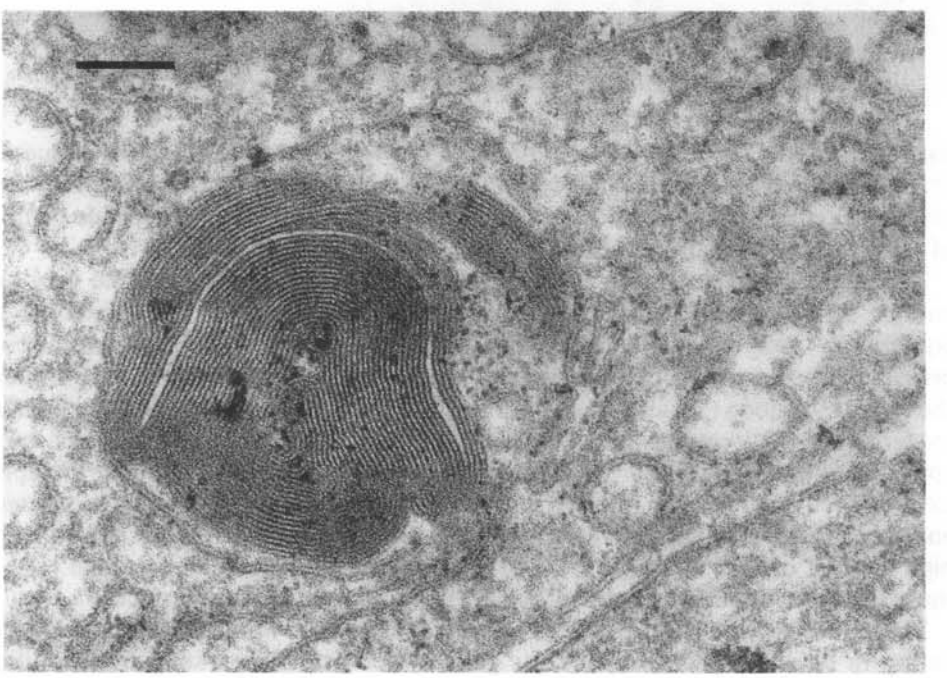

FIG. 4—One of the lamellar bodies seen in Fig. 3 shown at higher magnification. *Note* the highly lamellated structure and the solid core typical of an lamellar bodies (17). *Bar* = 100 nm.

FIG. 5—A magnified view of an oligolamellar vesicle and other osmiophilic inclusions in spinal cord such as shown in Fig. 3. These have hollow cores and, in some instances, seem to provide an oligolamellar lining to fluid-filled vacuoles. *Bar* = 1 μm.

basis (Table 1). The high concentration of phospholipid in both spinal tissue and brain is predictable because chloroform would be expected to elutriate DPPC from myelin sheaths as shown in Fig. 6. This would also explain the appreciable quantity of DPPC found in brain (Table 1).

The γ:A loops recorded on the Langmuir trough (Fig. 2) testify to the very high surface activity of the spinal extract, dropping surface tension immediately to the equilibrium value of 24 dyn/cm (27). Even pulmonary surfactant requires some compression of the monolayer before reducing surface tension appreciably and producing the typical γ:A loop (22) also shown in Fig. 2. In standard texts of physical chemistry, hysteresis in γ:A loops is attributed to lack of phase equilibrium, and the same would apply to phospholipid (29). The remarkably uniform surface tension of the spinal extract over such a large (5:1) area change would indicate very rapid recruitment and derecruitment of surfactant from the monolayer. This is consistent with the very high content of HP, and high HP:DPPC ratio, because it is well accepted (15, 19) that HP is most effective in recruiting DPPC to the air–liquid interface.

These properties of the HP–DPPC surfactant complex would certainly favor their ability to facilitate growth of the gas phase when gas is separating from solution. This is confirmed by the hydrophobic surface it can impart and the propensity to form bubbles, as shown in the simple ancillary experiment described above. It was

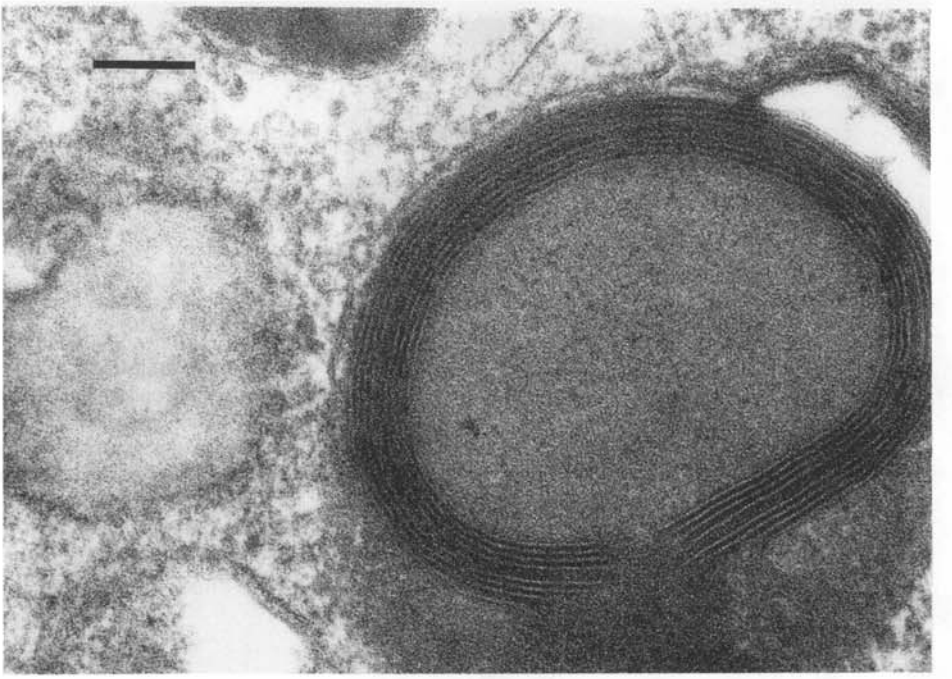

FIG. 6—A typical myelinated nerve axon in spinal cord shown for comparison purposes in which the myelin (predominantly SAPL) can be seen to be densely osmiophilic. *Bar* = 100 nm.

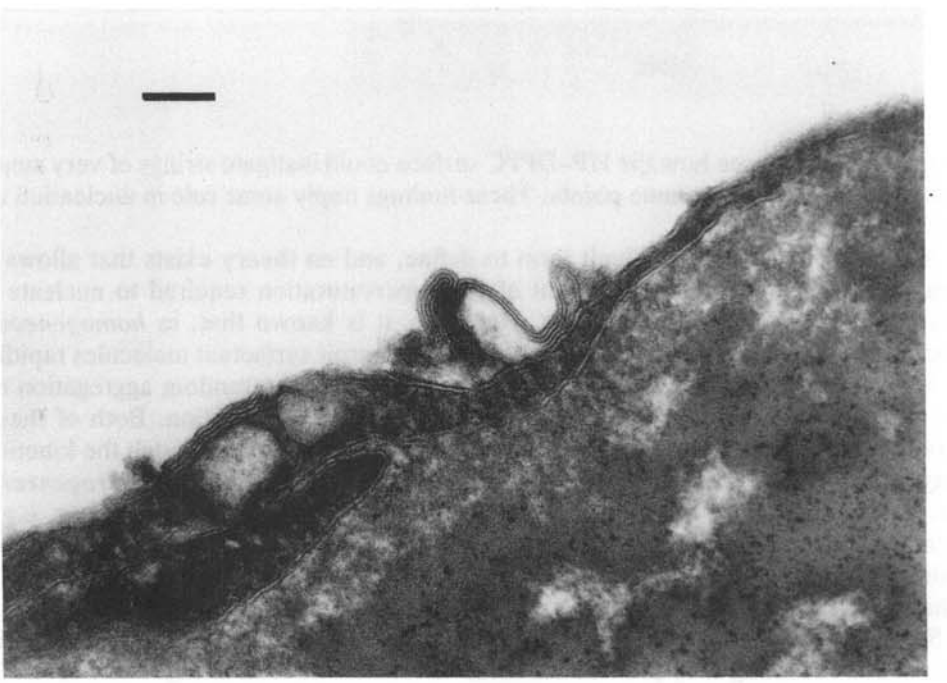

FIG. 7—Another view of cerebral endothlium showing both the oligolamellar luminal lining and a lamellated body attached to the endothelial cell, possibly in a state of unraveling. *Bar* = 100 nm.

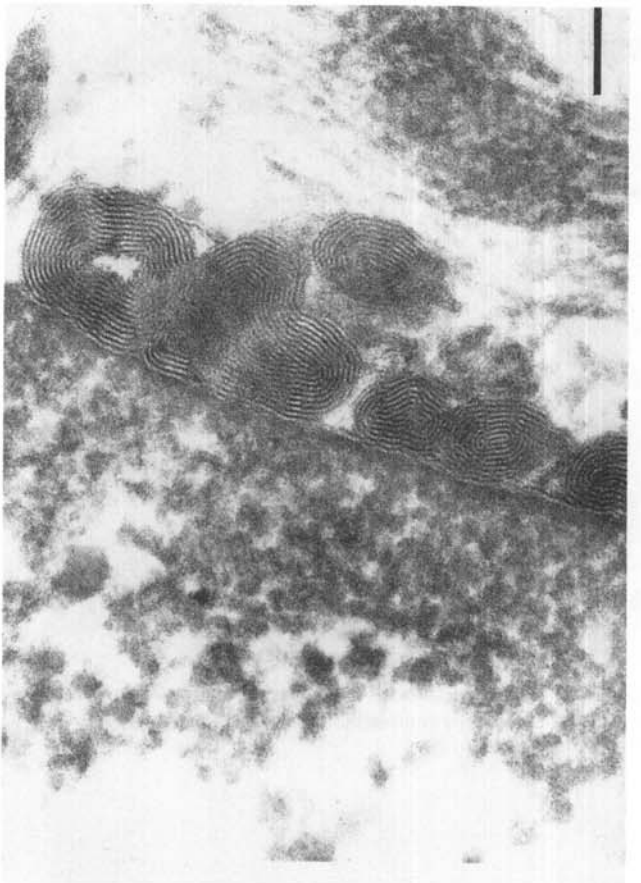

FIG. 8—A magnified view of sheep cerebral endothelium showing a "chain" of lamellar bodies attached to the vascular luminal surface, possibly in the process of forming the hydrophobic oligolamellar endothelial lining reported previously (28). *Bar* = 100 μm.

also interesting to see how the HP–DPPC surface could instigate strings of very small bubbles rising from the same points. These findings imply some role in nucleation as well as bubble growth.

A bubble nucleus is a difficult term to define, and no theory exists that allows a quantitative prediction of the extent of gas supersaturation required to nucleate a gas phase, even in pure water (30). However, it is known that, in *homogeneous* nucleation (30), surface tension and the ability to recruit surfactant molecules rapidly to the gas surface of any transient cavity occurring by the random aggregation of gas molecules in solution are important parameters in stabilization. Both of these properties are provided by the DPPC–HP surfactant complex, although the kinetics may still not be fast enough. Regarding the more likely scenario of *heterogeneous* nucleation, the DPPC–HP complex has a capability to bind to tissue surfaces, e.g., to macrophages (31), and for unraveled lamellar bodies to deposit an oligolamellar lining onto tissue surfaces, e.g., cerebral endothelium (28) or gastric mucosa (32), which would render them hydrophobic and conducive to bubble inception.

Since these oligolamellar linings are usually hydrophobic (28, 33), it is interesting to observe the lining they provide for some vacuoles—as seen in Fig. 5 and recently reported in esophageal epithelium (34)—in view of the interest in these sites for bubble formation (35). It is possible that the oligolamellar vesicles seen in Fig. 5 are

artifact, but lamellar bodies (Figs. 3 and 4) have never been reported as artifact (36). Some pathologists may tend to dismiss them as "the membranous remains of dead cells," but this would not seem to be the case, especially in the lung (17).

If lamellar bodies hold the potential for bubble formation, either directly or indirectly, then it is most tempting to speculate that their ratio in spinal:brain tissue (roughly 4:1) is responsible for the 3:1 ratio in spinal:cerebral symptoms of DCS often quoted (5). This ratio of symptoms agrees very closely with those of both HP and DPPC between those organs, and the data in Table 1 might also explain why skeletal muscle is very rarely involved in decompression-related illness.

Although the degree of coincidence of these ratios could be fortuitous, it is still proposed that the surfactant (DPPC–HP) complex is the agent that places the spinal cord so much at risk of decompression injury. If this hypothesis is correct, then the offending bubbles in the spinal cord should form where most lamellar bodies are found, i.e., in extravascular (largely perivascular) sites in the white matter. This would seem highly compatible with the demonstration of space-occupying lesions (SOLs) in the spinal white matter of decompressed dogs (9, 37, 38) and the fact that these lesions are gas-filled (37, 39), thus imparting the characteristic fulminant or "teased" appearance originally reported by Blick (2). It is interesting that myelin figures have been reported at the bubble surface (38) because these are well accepted in the lung (40) as an intermediate step in the unraveling of lamellar bodies on contact with a gas–aqueous interface.

This study tends to support the somewhat different nature of the lesions occurring in the brain and spinal cord. Several studies (41) have shown that air embolism produces pathology in the spinal cord quite unlike that produced by decompression, whereas spinal symptoms and their repeated reversal would favor the autochthonous bubble (10, 41) and, hence, the model reproduced in Fig. 9. Cerebral symptoms, by

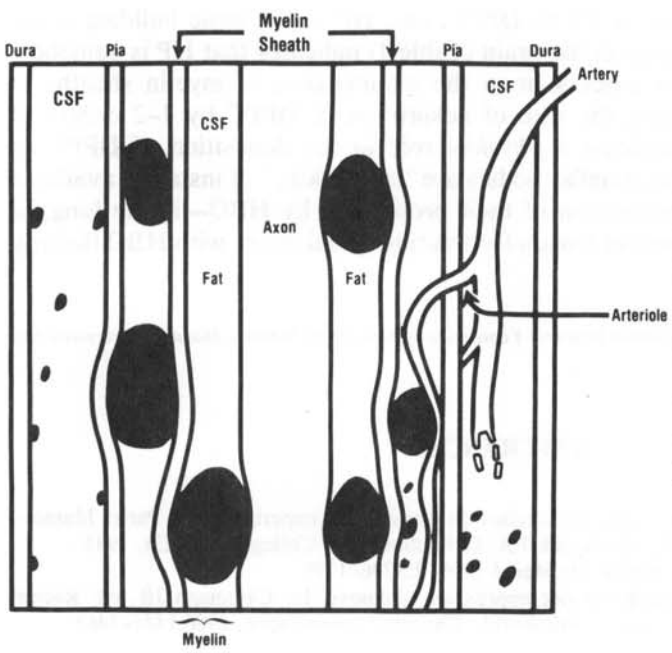

FIG. 9—Model of autochthonous bubbles pressing on arterioles to compromise blood flow as reproduced from Hills and James (10). Any global elevation of pressure by raised CSF pressure or formation of sufficient bubbles in more distant sites to cause distension of the pia would augment the pressure generated by local bubbles. This could elevate the net pressure opposing the vascular pressure in determining closure according to the "waterfall" concept.

comparison, would seem to be caused by intravascular events. This could take the form of either direct infarction, as proposed originally for the CNS as a whole (1, 4), or by circulating emboli compromising the blood–brain barrier (28, 42, 43). Hence it could be particularly significant that *intravascular* lamellar bodies were found in the brain (Figs. 5 and 8), in partial association with the oligolamellar endothelial lining reported earlier (28, 44) but *not* in the cord. Clearly, further studies are needed to determine the relative prepondence of HP in gray and white matter in both spinal and cerebral tissue and to determine any association with myelin.

If the hypothesis is correct that autochthonous bubbles are responsible for spinal DCS, this raises the issue of how such bubbles can result in spinal cord dysfunction for which Francis et al. (38) have listed three possible mechanisms. These are physical destruction of nerve fibers by bubble formation, ischemia, and chemical interactions, to which list can be added the competition of the bubble surface for surfactant present as myelin. This study has demonstrated the presence of far more lamellar bodies than needed to nucleate the bubbles that could cause the 30–100% disruption of fibers required to produce the degree of spinal dysfunction observed in dogs (38). However, the repeated *reversibility* of spinal symptoms returns this writer yet again to the ischemic mechanism proposed originally (10). Although the experimental evidence for that "waterfall" approach involved the global generation of extravascular pressure, closure of vessels by autochthonous bubbles had to be local to explain why not all nerve tracts are affected, and this was reflected in the original model proposed (10) and reproduced as Fig. 9. Thus, the watershed zones T4 and L1 with the lowest perfusion pressure would be at the greatest risk. Any generation of a global pressure, e.g., by elevation of cerebral spinal fluid (CSF) pressure, would exacerbate the situation by elevating the effective pressure with which the autochthonous bubble(s) are pressing on arterioles.

The fascinating question that this study poses is why there should be so much hydrophobic protein normally present in the spinal cord and what function it could serve. The fact that the ratio of HP to DPPC, i.e., HP to the basic building block of myelin, is virtually the same in the brain (Table 1) indicates that HP is somehow involved in the myelination process or in the maintenance of myelin sheaths in general. Its ability to increase the rate of adsorption of DPPC by 1–2 orders of magnitude (15, 19) could indicate a *physical* role in the deposition of DPPC as myelin. It is conceivable that lamellar bodies are "repair kits" of instantly available surfactant, in which case promotion of their production by HBO—in the lung, at least (45)—could provide another reason for treating spinal injury with HBO therapy (46).

This work was kindly funded by the Spinal Research Foundation of New South Wales.—*Manuscript received July 1992; accepted September 1992.*

REFERENCES

1. Bert P. La pression barometrique; récherches de physiologie experimentale. Paris: Masson. Translated by Hitchcock MA, Hitchcock FA. Columbus, OH: College Book Co, 1943.
2. Blick G. Notes on divers paralysis. Br Med J 1909; 2:1796–1799.
3. Palmer AC. The neuropathology of decompression sickness. In: Cavanagh JB, ed. Recent advances in neuropathology, vol. 3. Edinburgh: Churchill Livingstone, 1986:1441–1462.

4. Boycott AE, Damant GCC, Haldane J.S. The prevention of compressed air illness. J Hyg 1908; 8:342-443.
5. Hallenbeck JM, Bove AA, Elliott DH. Mechanisms underlying spinal cord damage in decompression sickness. Neurology 1975; 25:308–316.
6. Kety SS. The cerebral circulation. In: Field J, Magoun HW, Hall VE, eds. Handbook of physiology section 1: Neurophysiology. Baltimore: Williams & Wilkins, 1960:1751-1960.
7. Hales JR, Yeo JD, Stabback S, Fawcett AA, Kearns R. Effects of anesthesia and laminectomy on regional spinal cord blood flow in conscious sheep. J Neurosurg 1981; 54:620–626.
8. Blackwood W. Discussion on vascular disease in the spinal cord. Proc R Soc Med 1958; 51:543–547.
9. Francis TJR, Pezeshkpour GH, Dutka AJ. Arterial gas embolism as a pathophysiologic mechanism for spinal cord decompression sickness. Undersea Biomed Res 1989; 16:439–451.
10. Hills BA, James PB. Spinal decompression sickness: mechanical studies and a model. Undersea Biomed Res 1982; 9:185–201.
11. Golding FC, Griffiths P, Paton WDM, Walder DN, Hempleman HV. Decompression sickness during construction of the Dartford Tunnel. Br J Ind Med 1960; 17:167–180.
12. Grulke DC, Hills BA. Experimental cerebral air embolism and its resolution. In: Shilling CW, Beckett MW, eds. Underwater physiology VI. Proceedings of the sixth symposium on underwater physiology. Bethesda, MD: Undersea Medical Society, 1978:587–594.
13. Waite CL, Mazzone WF. Greenwood ME, Larsen R.T. Cerebral air embolism. I. Basic studies. Report 493, US Naval Submarine Medical Center, Groton, CT, 1967.
14. Hills BA. A thermodynamic and kinetic approach to decompression sickness. Adelaide: Libraries Board of South Australia, 1966.
15. Hawgood S, Benson BJ, Schilling J, Damm D, Clements JA, White RT. Nucleotide and amino acid sequences of pulmonary surfactant protein SP18 and evidence for cooperation between SP18 and Sp28-36 in surfactant lipid adsorption. Proc Natl Acad Sci USA 1987; 84:66–70.
16. Oosterlaken-Dijksterhuis MA, van Eijk M, van Buel BL, van Golde LMG, Haagsman HP. Surfactant protein composition of lamellar bodies isolated from rat lung. Biochem J 1991; 274:115–119.
17. Stratton CJ. Morphology of surfactant producing cells and of the alveolar lining layer. In: Robertson B, van Golde LMG, eds. Pulmonary surfactant. Amsterdam: Elsevier, 1984:68–118.
18. King RJ, Clements JA. Surface active materials from dog lung. II. Composition and physiological correlations. Am J Physiol 1972; 223:715–726.
19. Hawgood S, Haagsman HP. Surfactant-associated protein A. In: Ekelund L, Jonson B, Malm L, eds. Surfactant and the respiratory tract. Amsterdam: Elsevier, 1989:57–74.
20. Allen G. Sequencing of proteins and peptides. In: Burdon RH, Knippenberg PH, eds. Laboratory techniques in biochemistry and molecular biology, vol. 9. Amsterdam: Elsevier, 1968.
21. Moore S, Stein WH. Photometric ninhydrin method for use in the chromatography of amino acids. J Biol Chem 1948; 176:367–388.
22. Clements JA. Surface tension of lung extracts. Proc Exp Biol Med 1957; 95:170–172.
23. Ueda S, Kawamura K, Ishii N, et al. Ultrastructural studies on surface lining layer of the lungs, part IV. Resected human lung. J Jpn Med Soc Biol Interface 1985; 16:34–60.
24. Kalina M, Pease DC. The preservation of ultrastructural saturated phosphatidyl cholines by tannic acid in model systems and type II pneumocytes. J Cell Biol 1977; 74:726–741.
25. Rouser G, Siakotos AN, Fleischer S. Quantitative analysis of phospholipids by thin-layer chromatography and phosphorus analysis of spots. Lipids 1966; 1:85–86.
26. Possmayer F, Yu SH, Schurch S. Biophysical properties of pulmonary surfactant. In: Ekelund I, Jonson B, Malm L, eds. Surfactant and the respiratory tract. Amsterdam: Elsevier, 1989:39–55.
27. Bangham AD, Morley CJ, Phillips MC. The physical properties of an effective lung surfactant. Biochim Biophys Acta 1979; 573:552–556.
28. Hills BA. A hydrophobic oligolamellar lining to the vascular lumen of some organs. Undersea Biomed Res 1992; 19:107–120.
29. Mingins J, Taylor JAG. Physicochemical properties of phospholipid monomolecular layers. Proc R Soc Med 1973; 66:383–385.
30. Hemmingsen BB. Intracellular gas supersaturation tolerances. In: Brubakk AO, Hemmingsen BB, Sundnes G, eds. Supersaturation and bubble formation in fluids and organisms. Trondheim: Tapir, 1989:105–123.

31. van Iwaarden F, Welmers B, Verhoef J, Haagsman HP, van Golde LM. Pulmonary surfactant protein 'A' enhances the host defence mechanism of rat alveolar macrophages. Am J Respir Cell Mol Biol 1990; 2:91–98.
32. Hills BA. A physical identity for the gastric mucosal barrier. Med J Aust 1990; 153:76–81.
33. Hills BA, Butler BD, Lichtenberger LM. Gastric mucosal barrier hydrophobic lining to the lumen of the stomach. Am J Physiol 1983; 7:G561–568.
34. Spychal RT, Kwun SY, Watson A. Ultrastructural identification of surfactant-like material in human oesophageal mucosa. J Gastroenterol Hepatol 1992; 7:A19.
35. Walsby AE. The gas vesicle: a stable gas-filled structure in bacteria. In: Brubakk AO, Hemmingsen BB, Sundnes G, eds. Supersaturation and bubble formation in fluids and organisms. Trondheim: Tapir, 1989:69–104.
36. Crang RFE, Klomparens KL. Artifacts in biological electron microscopy. New York: Plenum Press, 1988.
37. Hardman JM, Beckman EL. Pathogenesis of central nervous system decompression sickness. Undersea Biomed Res 1990; 17(suppl):95–96.
38. Francis TJR, Griffin JL, Homer LD, Pezeshkpour GH, Dutka AJ, Flynn ET. Bubble-induced dysfunction in acute spinal cord decompression sickness. J Appl Physiol 1990; 68: 1368–1375.
39. Burns BA, Hardman JM, Beckman EL. In situ bubble formation in acute central nervous system decompression sickness. J Neuropathol Exp Neurol 1988; 47:371.
40. Sanderson RJ, Vatter AE. A mode of formation of tubular myelin from lamellar bodies in the lung. J Cell Biol 1977; 74:1027–1031.
41. Francis TJR, Pezeshkpour GH, Dutka AJ, Hallenbeck JM, Flynn ET. Is there a role for the autochthonous bubble in the pathogenesis of spinal cord decompression sickness. J Neuropathol Exp Neurol 1988; 47:475–487.
42. Gorman DF, Browning DM. Cerebral vasoreactivity and arterial gas embolism. Undersea Biomed Res 1986; 13:317–335.
43. Hills BA, James PB. Microbubble damage to the blood–brain barrier: relevance to decompression sickness. Undersea Biomed Res 1991; 18:111–116.
44. Hills BA. A physical identity for the blood–brain barrier. Proc R Soc NSW 989; 122:13–29.
45. Clark JM, Lambertsen CJ. Pulmonary oxygen tolerance and the rate of development of pulmonary oxygen toxicity in man at two atmospheres inspired oxygen tension. In: Lambertsen CJ, ed. Proceedings of the third symposium on underwater physiology. Baltimore: Williams & Wilkins, 1967:439–451.
46. Kelly DL Jr, Lassiter RL, Calogero JA. Effects of hyperbaric oxygenation and tissue oxygen studies in experimental paraplegia. J Neurosurg 1972; 36:425–429.